Neuroscience 352 (2017) 226–235

TACTILE OBJECT CATEGORIES CAN BE DECODED FROM THE PARIETAL AND LATERAL-OCCIPITAL CORTICES

RAÚL HERNÁNDEZ-PÉREZ,* LAURA V. CUAYA EDUARDO ROJAS-HORTELANO, AZALEA REYES-AGUILAR, LUIS CONCHA AND VICTOR DE LAFUENTE*

Instituto de Neurobiología, Universidad Nacional Autónoma de México, Querétaro, QRO. 76230, Mexico

Abstract—The visual system classifies objects into categories, and distinct populations of neurons within the temporal lobe respond preferentially to objects of a given perceptual category. We can also classify the objects we recognize with the sense of touch, but less is known about the neuronal correlates underlying this cognitive function. To address this question, we performed a multivariate pattern analysis (MVPA) of functional magnetic resonance imagining (*f*MRI) activity to identify the cortical areas that can be used to decode the category of objects explored with the hand. We observed that tactile object category can be decoded from the activity patterns of somatosensory and parietal areas. Importantly, we found that categories can also be decoded from the lateral occipital complex (LOC), which is a multimodal region known to be related to the representation of object shape. Furthermore, a hyperalignment analysis showed that activity patterns are similar across subjects. Our results thus indicate that tactile object recognition generates category-specific patterns of activity in a multisensory area known to encode objects, and that these patterns have a similar functional organization across individuals.

Key words: tactile, somatosensory, perception, multivariate pattern analysis, object recognition, object category.

INTRODUCTION

The ventral stream of the cortical visual system contains neural representations of visual objects such as faces, animals, and inanimate objects. Thus, an organizing principle of the visual system is the neural encoding of abstract categories of behaviorally relevant objects (Kiani et al., 2007; Meyers et al., 2008; Freeman and Simoncelli, 2011; Lehky et al., 2014; Aparicio et al., 2016). It is well established that these neuronal representations are invariant to changes in low-level physical characteristics such as luminance, contrast, angle of view, location, or size. Moreover, it has been observed that some of these circuits encode representations that are invariant to the sensory modality used to recognize the objects, i.e., a given object elicits similar patterns of neuronal activity irrespective of the object being recognized by visual, auditory, or tactile cues (Amedi et al., 2001; Grill-Spector et al., 2001; Ghazanfar and Schroeder, 2006; Kassuba et al., 2011; Man et al., 2015). These unified neuronal representations correspond closely with the unified and stable subjective perception that we have of the objects around us.

In the somatosensory system, the different physical attributes that define a tactile object, such as texture, curvature, or edge orientation, are encoded in the neuronal activity of numerous parietal areas that show varying degrees of selectivity for those features (Bodegård et al., 2001; Iwamura, 1998; Sathian, 2016; Yamada et al., 2016; Yau et al., 2009, 2016). Peripheral receptors and areas 1 and 3b, for example, contain neurons that are selective for the orientation of edges (Bensmaia et al., 2008; Pruszynski and Johansson, 2014; Peters et al., 2015); area SII contains neurons that show orientation selectivity across several finger pads (i.e., they show positional invariance; Fitzgerald et al., 2006), and there is evidence that edge curvature is represented in area 2 (Yau et al., 2013).

However, it is not clear if these variate tactile attributes, which are encoded in separate neuronal populations at early processing stages, converge in upstream association areas to generate a unified representation of tactile objects. Moreover, it is important to know if such tactile category encoding is located within the somatosensory system itself or whether it is located within a multisensory association area. There is strong evidence that the object representations along the temporal lobe can be activated by more than one sensory modality (Kim and Zatorre, 2011; Lacey and Sathian, 2014; Podrebarac et al., 2014; Snow et al., 2014), and we know that visual information can transfer to the tactile modality and vice-versa (Yildirim and Jacobs, 2013). In particular, the lateral occipital complex (LOC) has been shown to encode objects that are identified by touch or sight (Amedi et al., 2002; Peltier et al., 2007; Stilla and Sathian, 2008; Lucan et al., 2010; Masson et al., 2015; Erdogan

*Corresponding authors. Addresses: Institute of Neurobiology, National Autonomous University of Mexico, Boulevard Juriquilla 3001, Querétaro, QRO. 76230, Mexico.
E-mail addresses: raul@lafuentelab.org (R. Hernández-Pérez), lafuente@unam.mx (V. de Lafuente).
Abbreviations: BOLD, blood-oxygen-level-dependent; *f*MRI, functional magnetic resonance imagining; LOC, lateral occipital complex; LSVM, linear support vector machine; M1, primary motor; MVPA, multivariate pattern analysis; SMA, supplementary motor area; V1, primary visual.

http://dx.doi.org/10.1016/j.neuroscience.2017.03.038
0306-4522/

et al., 2016). Pietrini and colleagues showed that the inferotemporal cortex generates neuronal representations of tactile objects and that these representations are similar to those generated by visually identifying the same objects (Pietrini et al., 2004).

The level of abstraction that follows object representation is object category, i.e., the representation of a group of objects that share a high-level attribute such as function (e.g., spoons or pens) or behavioral relevance (e.g., faces or animals). These categories have been described in the prefrontal, temporal and occipital lobes (Ishai et al., 2000; Kourtzi and Connor, 2011; Watanabe et al., 2012; McKee et al., 2014; Proklova et al., 2016). We seek to gather evidence on whether the cortical activity could be used to decode the category of an object explored with the sense of touch.

Recognizing and classifying the objects we touch is a fundamental cognitive skill that allows not only naming those objects, but more importantly, allows recovering stored relevant information related to the objects around us. Although objects vary considerably in their specific physical characteristics, classifying them into perceptual categories simplifies and organizes the sensory world around us. It allows planning our behavior and executing the motor commands to adequately interact with those objects. It is well established that subjects can correctly identify and categorize objects explored only with the sense of touch (for a recent review see Sathian, 2016). This can also be done by congenitally blind individuals, indicating that a visual representation of objects is not needed for identification or classification. A relevant question is thus what are the neuronal correlates of tactile object identification and, moreover, the neuronal correlates of tactile object categories.

The existence of neuronal representations of tactile categories would be consistent with the idea that the somatosensory system uses similar processing algorithms and strategies as the visual system, which hierarchically encodes object properties such as texture, form, object identity and finally, object category.

We performed a multivariate pattern analysis (MVPA) on block-design functional magnetic resonance imagining (*f*MRI) data to identify the cortical areas that contain enough information to decode tactile object categories significantly above chance (Hanke et al., 2009; Haxby et al., 2014). We probed the whole cortex with a searchlight analysis that selected the voxels within a sphere (radius = 3 voxels) to train a linear support vector machine (LSVM) to classify the activity associated with 10 types of objects that were explored with the right hand. Our results revealed voxel clusters in the parietal and the LOC from which the category of the touched objects could be decoded.

EXPERIMENTAL PROCEDURES

Stimuli and task design

Participants explored a total of 120 objects grouped into 10 categories comprising spoons, stuffed toys, bottles, pens, books, balls, strings, drinking glasses, pseudorandom 3D shapes, and square sandpapers with different roughness (12 different objects per category). The objects were explored for 3 s with the right hand, and participants performed a one-back repetition detection task in which they had to indicate whether the object they explored was the same or different from the previous one. After the 3 s exploration period the object was removed and the participants had a 1 s window to press one of two buttons with their left hand to indicate whether the object was the same or different from the previous one.

A *block* consisted of six stimuli of the same category (Fig. 1). Blocks of different object categories were selected in pseudo-random order, lasted 24 s each, and were separated by a 12 s baseline. The stimuli in each block were selected with a 50% chance of being the same as the previous one. A presentation of 10 different blocks defined a *run*, and subjects performed 12 repetition runs that lasted 372 s each. Participants were given a 15 min break after six runs.

Subjects lay within the scanner with their right palm up and the experimenter handed them the objects following instructions from a computer monitor about the time and the object to be handled. The participants were instructed to close their eyes within the scanner and held a button pad with their left hand to press one of two buttons to indicate whether the current object was the same or different from the previous one. The objects we used were visible to the participants before and after completion of the scans. We did not attempt any systematic selection of object categories, and our criterion was straightforward: we selected common objects that could be comfortably manipulated with one hand and that were compatible with MRI. Only one category (the 3D random shapes that we used in a previous study, Rojas-Hortelano et al., 2014) contained non-familiar objects. We measured volume, weight and compliance (using von Frey filaments) of each object. Mean object volume was 251 cm^3, mean weight 60 g, and mean compliance of non-rigid objects was 2 N.

Subjects and Image acquisition

Ten healthy right-handed subjects (5 women, age range 27–36 yr) underwent *f*MRI on a 3-T Phillips Achieva TX scanner (Best, The Netherlands) using an echo planar imaging gradient echo (EPI-GRE) sequence with a repetition time (TR) of 2 s and an echo time (TE) of 27 ms. Functional volumes consisted of 32 axial slices covering the whole brain with a voxel size resolution of $2 \times 2 \times 3.5\ mm^3$. On each of the 12 repetition runs 190 volumes were acquired. Subjects gave written consent and were compensated for their time. Experimental procedures were approved by the institutional Research Ethics Committee and were in accordance with the Declaration of Helsinki.

Data preprocessing and pattern analysis

Data preprocessing was performed with FSL (FMRIB's Software Library; www.fmrib.ox.ac.uk/fls). Each run was motion-corrected to the first volume of each participant. No smoothing or filtering was applied. Images were

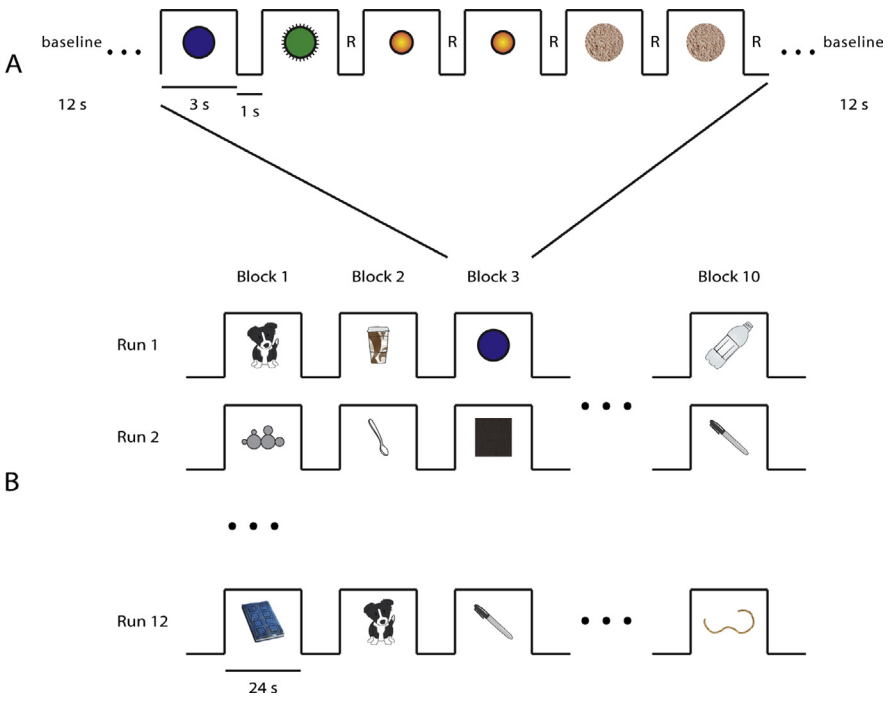

Fig. 1. Task design. (A) Participants explored an object with their right hand for 3 s and had to indicate whether it was the same or different from the previous object. A 1 s window separated each stimulus presentation during which subjects pressed one of two buttons with their left hand to communicate their decision (*R*). (B) Six stimulus presentations of the same category defined a *block*, and 10 blocks of the different object categories constituted a *run*. A total of 12 repetition runs were collected in the *f*MRI session of each participant. Each block lasted 24 s and were separated by a 12 s baseline period.

brain-extracted and temporally realigned. MVPA was performed using the PyMVPA software package (Hanke et al., 2009) and the LibSVM's implementation of the LSVM (www.csie.ntu.edu.tw/~cjlin/libsvm). We used the multi-class classification implemented in the PyMVPA package. The particular algorithm, called "boosting" uses meta-classifiers that are formed from basic classifiers and then used to forma a meta-prediction (Connolly et al., 2016; Hanke et al., 2009).

Previous to the MVPA, the events in each run were time-shifted 6 s to account for the hemodynamic response. Each run was linearly detrended, Z-scored, and had the baseline volumes removed. The blood-oxygen-level-dependent (BOLD) signal of each voxel was averaged over the 24 s duration of each stimuli block (a 24 s block contained six stimuli of the same category; Fig. 1). We performed a 10 way classification in which the LSVM classifier had to choose among the 10 possible categories for the prediction. The classifier performance was calculated by adding the number of correct classifications divided by the total number of classification attempts. A full-brain searchlight analysis was performed using a 3-voxel radius, and an LSVM classifier was used to assess whether object category could be differentiated by the patterns of BOLD activity in the voxels within the searchlight sphere (Pereira and Botvinick, 2011). In the searchlight analysis, each voxel was selected along with a sphere of voxels around it. The BOLD signal in these voxels (the mean activity across the 24-s block duration) was used to train the LSVM classifier to measure the accuracy with which the sphere of voxels could predict the different object categories. The accuracy of the sphere then becomes the accuracy of the voxel at the center (Etzel et al., 2013). We illustrate the effect on accuracy of using different radiuses for the searchlight analysis (Fig. 5), but for all the analyses and statistical calculations we used a 3-voxel radius.

The classifier performance for each sphere of voxels was estimated using a leave-one-out cross-validation scheme. This consisted in training the classifier using all but one experimental run and then predicting the object category of that test run. A different test run was then selected and the classifier was then re-trained with the remaining runs. The procedure was repeated until all runs were used once as the test run. This was repeated for every voxel in the brain, resulting in a spatial map of prediction accuracy. A map of accuracy was created for each participant.

The single-subject maps were thresholded with the binomial test to show the voxels whose probability of identifying the object categories was significantly above chance level ($p < 0.01$; chance level is 1/10). For the 120 trials distributed over 10 categories the expected chance outcome is 12 correct trials. The binomial test tells us that 20 or more correctly classified trials are significantly above chance, and that corresponds to a performance accuracy of 20/120 = 0.167, which is the cutoff level depicted in the color scale of Fig. 3. In order to estimate the cluster size expected by chance we selected the sphere with the best performance in a given participant, and calculated the performance under a no-signal condition, in which the category labels were randomized in the runs used to train the classifier. We repeated this process 1000 times. This provided us with an expected performance distribution. We created 1000 new single-subject maps for each run by taking random samples from the created distribution. These provide us with performance maps under a no-signal condition. From these maps, we calculated the cluster sizes expected by chance and use them to correct the single-subject maps ($p < 0.01$).

To identify the informative voxels across subjects (group analysis) we transformed each subject's map to the MNI-152 standard space and applied a binomial test on the pooled trials to filter out the voxels that did not surpass the 0.1 chance probability value. After this, we performed a *t*-test on each voxel of this standard map (cut-off value $t(9) = 2.82$; $p = 0.01$; Fig. 4), correcting

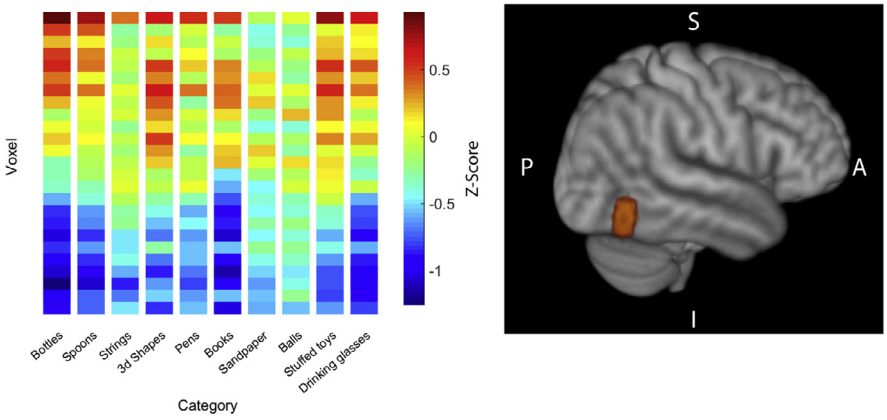

Fig. 2. Example data. The mean BOLD signals of 25 voxels from a mask over the lateral occipital complex (LOC) of one subject are shown for each object category (Z-score, voxels were selected from an ANOVA-based feature selection ranking). The LSVM algorithm is trained to classify the spatial pattern of activity associated with each category and its accuracy is then measured by classifying data on which it was not trained.

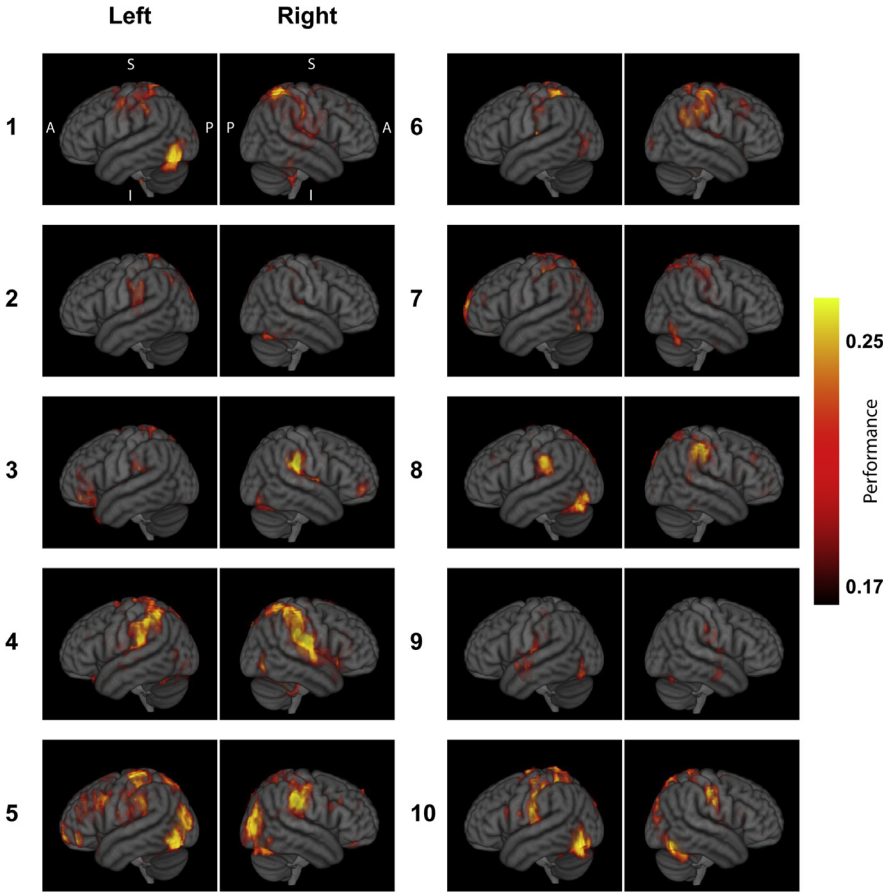

Fig. 3. Single-subject prediction accuracy maps. The prediction accuracy (probability of correct classification) at each voxel is shown in color and was calculated from a sphere of voxels around it (radius = 3, searchlight analysis). Only voxels with accuracy above chance level are shown ($p < 0.01$, binomial test, cluster-corrected). Individual maps were transformed to the MNI-152 atlas. Note that although significant variability is observed between participants, informative voxels are consistently observed in the parietal, and temporo-occipital cortices.

for multiple comparison with the False Discovery Rate method ($p < 0.01$). Finally, we performed cluster correction on the group-level map by randomly shuffling the categories labels (Monte Carlo permutation testing, 1000 permutations). This group analysis resulted in a new map showing the significant t-static value (Fig. 4) of performance accuracy across participants.

For the hyperalignment analysis, masks in the parietal and the LOC were used to select the voxels that were analyzed using the methods described by Haxby et al., (2011) with the PyMVPA software package (Hanke et al., 2009). Briefly, hyperalignment is a method that aligns participants' data in a common high-dimensional space in order to evaluate the extent to which activity patterns are consistent across subjects. For this, the activity of the voxels selected from the masks is represented as a high-dimensional vector (a dimension for each voxel), and a transformation matrix is used to rotate the vector such that distances between vectors are minimized (one vector for each stimulus category). This creates what is called a *common model space* that represents the activity associated with each object category across subjects. The LSVM classifier is then trained to classify the object categories using the aligned activity, and its accuracy is tested on the activity of each participant in a leave-one-out scheme. The result of this analysis is an accuracy estimate with which the category of a tactile object can be decoded from the activity of one subject using what the classifier learned from the other subjects. We used 300 voxels selected from an ANOVA and ranked them according to their modulation across the ten object categories (ANOVA-based feature selection ranking). We avoided double-dipping by leaving the subject to be tested out of the voxel selection.

RESULTS

The participants explored the objects with their right hand and successfully performed the one-back same-different task with an overall 90.4% of correct responses (±1% s.e.; chance performance is 50%). This behavioral result confirms that subjects were attending to the stimuli and were using tactile information to determine whether two

consecutively presented objects were the same or different (Fig. 1). We found no differences in the percentage of correct responses across object categories ($p = 0.57$, Friedman test). This is an important result because it rules out that differences in task difficulty across categories (and not tactile properties) might have helped the LSVM classifier to distinguish between objects.

We used a MPVA searchlight analysis to identify the brain areas with activity patterns that were significantly informative about object categories. An example of the raw data that were used to train the LSVM classifier is illustrated in Fig. 2, where the BOLD signals of 25 voxels from the LOC are shown for the different object categories that a participant explored. The different spatial patterns, induced by the different object categories, are used by the LSVM classifier to predict the objects that participants touch. Although there might appear that some object categories share similarities in their pattern of cortical activation, a representation similarity analysis (RSA) failed to reveal any meaning pattern, i.e., we could not establish a hierarchical arrangement of the evoked neuronal activity.

The voxels that are significantly informative about tactile category are shown in single-subject maps in Fig. 3 ($p < 0.01$, corrected for multiple comparisons; see Methods). The results illustrate that although a considerable amount of variability exists between subjects, there are informative clusters consistently located in the parietal and temporo-occipital regions. These single-subject maps demonstrate that prediction accuracies can reach 25%, well above the 10% chance accuracy expected from classifying 10 categories.

The brain regions that were consistently predictive across subjects were identified by a group analysis that marked the voxels with prediction accuracy significantly above chance ($p < 0.01$; see Methods). This group analysis revealed that the category of tactile objects can be decoded from the activity of two bilateral cortical clusters: one is a large cluster spanning the anterior and posterior parietal lobes, and the other is a smaller cluster located in the lateral-occipital regions of both hemispheres (Fig. 4).

To test the generality of these results we used a different classifier algorithm called k-Nearest-Neighbor (kNN) and found that although the general accuracy was ~20% lower with this classifier, the results are similar in the sense that both areas are informative about object category and the parietal areas have larger prediction accuracy.

To estimate the variability in classification accuracy that can be expect by chance we carried a Monte Carlo permutation testing in which we randomly shuffled object categories and recalculated the classification accuracy (1000 repetitions). The distribution of accuracies is plotted in Fig. 6 and it shows that the chance of obtaining a classification accuracy larger than 0.18 is less than 0.01. Importantly, the accuracy from shuffled data never reached the peak accuracies of LOC and parietal cortices, so the statistical significance of the results are at least $p < 1e{-}3$. This result demonstrates that our results are significantly above chance and above the noise expected from the intrinsic variability in the BOLD signal.

It is known that the number of informative voxels increases when a larger searchlight radius is used (Etzel et al., 2013). To explore this effect, we calculated the significantly informative voxels, at group level, for radiuses of 2–5 voxels (Fig. 5). The results of this analysis show that, as expected, the extension of the informative clusters grows in proportion to the radius used in the searchlight procedure. We note, however, that the location of the most significantly informative clusters (t-score > 5) remains centered in the parietal and lateral temporo-occipital cortices. As Fig. 5 shows, the searchlight with radiuses 4 and 5 revealed that the posterior end of the supplementary motor area (SMA) is also informative about object category. This observation is consistent with previous research indicating that the SMA is engaged in tactile object recognition (Reed et al., 2004). The figure also shows small changes in the location of peak significance and this is an expected result arising from incorporating new voxels into the training of the classifier and the calculation of accuracy.

After having identified the parietal and the temporo-occipital regions as informative about the object category we then wanted to compare the prediction accuracy between these two cortical regions, and also estimate how this accuracy changes as a function of the number of voxels used to train the LSVM classifier. The voxels were selected from bilateral masks covering the parietal lobes and the LOCs, and they were added according to an ANOVA-based feature selection ranking. The results shown in Fig. 6 demonstrate that, for any given number of voxels, the parietal lobe has a greater capacity to identify object category as compared to the LOC region. Prediction accuracy peaks at around 10^2 voxels for both areas. Given that the LOC and parietal cortices have different intrinsic sizes, this analysis shows that the parietal cortex has a larger accuracy in predicting object categories even when controlling for the number of voxels. We

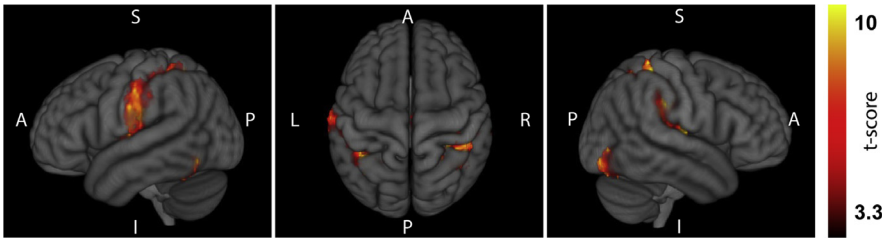

Fig. 4. Object category could be predicted from clusters located over the parietal and temporal-occipital cortices. The significantly informative voxels across participants ($p < 0.01$, t-test, FDR and cluster-corrected) are shown over lateral and superior views of the MNI-152 atlas. Color denotes the t-score of the test at the group level ($n = 10$ participants). (For interpretation of the references to colour in this figure legend, the reader is referred to the web version of this article.)

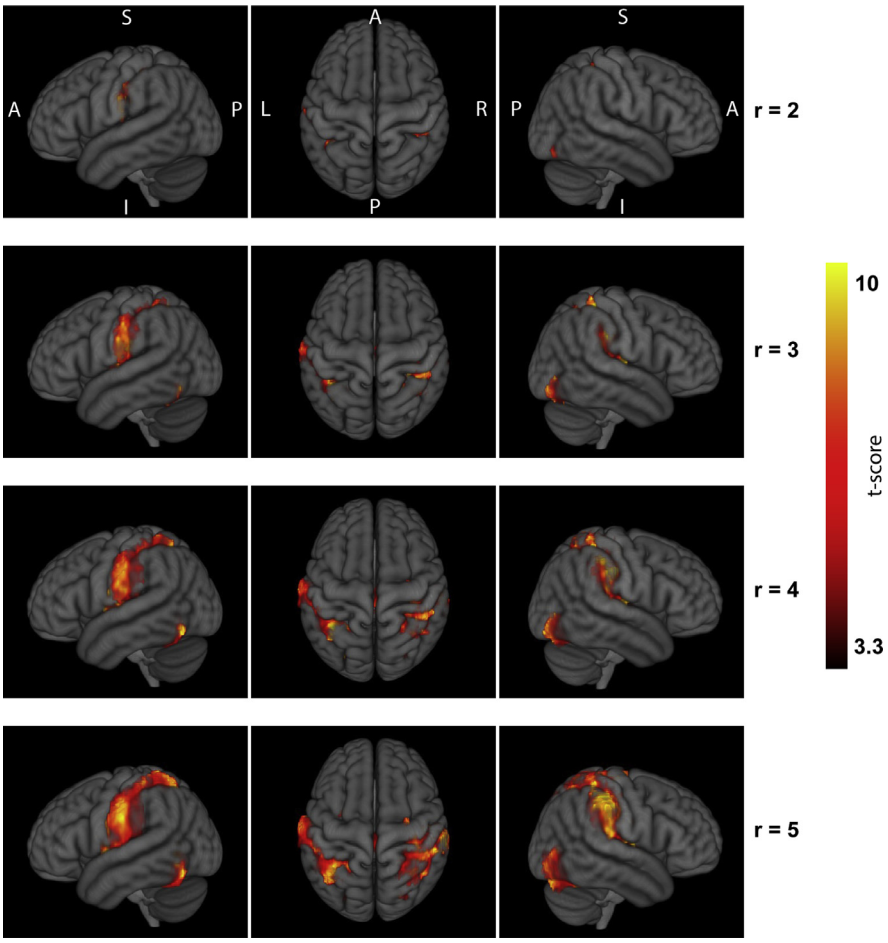

Fig. 5. The extension of the informative regions grows as a function of the searchlight radius (one row for each radius, indicated by r). The significantly predictive voxels are shown in color over lateral and superior view of the MNI-152 atlas. Note that although the area of significantly informative regions is dependent on the radius of the searchlight sphere, the clusters remain centered on the parietal and temporo-occipital lobes. (For interpretation of the references to colour in this figure legend, the reader is referred to the web version of this article.)

additionally computed the accuracy of the combined areas and found that it was ~2% greater than that of the parietal cortices alone. We also conducted a psychophysical interaction analysis (PPI; Friston et al., 1997) by placing a seed (6 mm in diameter) in the left LOC (MNI coordinates $x = -56$, $y = -62$, $z = -8$) and found that during task execution the activity of LOC and parietal cortices (ventral portion) were negatively correlated ($p < 0.05$). This is an interesting finding that could be related to the different processing strategies that these cortices use during the tactile exploration task.

It is possible that one or two categories could be pushing discrimination accuracy up, with the rest of the categories being discriminated at chance level. To explore this possibility we plot the classifier accuracy for each category, for LOC and the parietal areas (Fig. 6B). It can be seen that, although there is a gap of ~40% between the highest and lowest category, instead of a few areas pushing general accuracy up there is a continuum of classification performance across categories.

Finally, we were interested in testing the extent to which the patterns of activity in the parietal and LOC regions are comparable across individuals. If the tactile exploration of objects were to generate a consistent pattern of activity across individuals, that would support the notion that the classifier is making use of physiologically relevant patterns inherent to the parietal and LOC cortices. To test this, we used a hyperalignment method in which the activity of the parietal and LOC regions of each subject was projected onto a high-dimensional space and then rotated to minimize the distance between the representations of the categories across subjects. The LSVM classifier was then trained on this hyperaligned activity, and the classification performance was tested on the activity of each participant. We trained the classifier with voxel activity from bilateral masks of the parietal and LOC regions of each participant in a leave-one-out cross-validation scheme. The results indicate that the hyperaligned patterns of activity can be successfully used to predict the categories of the objects that each participant is exploring (*t*-test, $p = 0.012$ for the LOC mask, $p = 4e{-}5$ for the parietal mask; 300 voxels were used from each mask). This evidence supports the notion that the exploration of tactile objects generates similar patterns of activity across subjects.

To test the specificity of the hyperalignment analysis we selected voxels from masks over the primary visual (V1) and primary motor (M1) areas and repeated the alignment procedure and classifier training. We found that V1 and M1 patterns of activity were not significantly informative of object category (V1 accuracy was 0.096, $p = 0.63$; M1 accuracy was 0.116, $p = 0.032$). It must be noted that M1 was close to statistical significance and this could be due to its close relationship with the parietal cortices that, as our results show, are informative about object category.

DISCUSSION

Our results demonstrate that the category of an object explored with the hand can be decoded significantly above chance from the pattern of activity of parietal and LOC cortices of both hemispheres. The decoding accuracy maps of single subjects show that there is considerable variability in the distribution of voxels that can be used to train the classifier. This may reflect differences in the perceptual and cognitive strategies

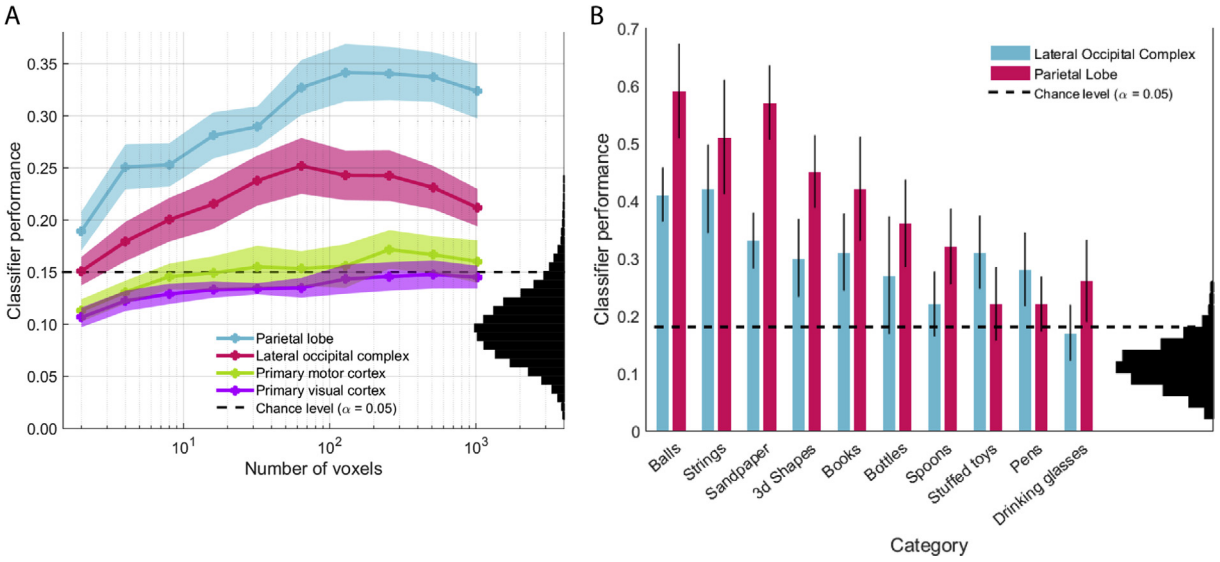

Fig. 6. (A) Classification performance is dependent on the number of voxels used to train the LSVM classifier. The order in which the voxels from the parietal and the lateral occipital complex (LOC) cortices are added was determined by ordering them according to an ANOVA-based feature selection ranking. The parietal cortex has larger predictive capacity for a given number of voxels as compared to LOC. The shaded region denotes standard error of the mean across subjects. The distribution on the right represents the classifier performance under a no-signal condition in which the category labels in the training set are randomly shuffled (Monte Carlo permutation test, 1000 repetitions). (B) All categories contribute to the general classification performance. The classification performance of each category was calculated from the bilateral masks of the lateral occipital complex and the parietal cortex for all participants ($n = 10$). Error bars denote standard error of the mean across subjects. The distribution shown in the right was calculated by randomly shuffling the categories before training the classifier in a permutation test (1000 repetitions).

that each participant uses to explore and identify the objects. Importantly, however, the group analysis revealed consistent informative clusters in the parietal and LOC cortices. Moreover, the patterns of activity in these predictive areas were similar across subjects as revealed by the hyperalignment method in which the activity of the group could be successfully used to decode the objects that single subjects were exploring. This result indicates that the functional representation of object category within this cortical region is shared among individuals.

It is important to note that the objects from the different categories have different shapes, weights, and textures, and it is likely that subjects used different hand movements to explore the objects of different categories (Thakur et al., 2008; Chen et al., 2009). The hand movements required to explore and recognize the shape of a spoon, for example, are different from those used to identify a stuffed toy. It is not surprising, then, that object categories can be decoded from the patterns of activity of the somatosensory areas (Gardner et al., 2007; Mollazadeh et al., 2014; Kim et al., 2015). A plausible explanation is that the activity of the somatosensory areas can be used to decode objects because different categories induce different exploratory movements and thus generate distinct streams of low-level physical information. The hyperalignment analysis supports this view as it revealed that M1 decoding accuracy was close to statistical significance ($p = 0.032$).

Although the predictive capacity of the somatic cortices might be due in part to different physical attributes and the different exploratory movements inherent to each type of object, we want to point out that accuracy levels are similar for both hemispheres (Fig. 5, bottom panels). If low-level attributes and hand movements were the only contributing factor to classification performance, we would have expected accuracy to be higher in the left hemisphere given that subjects explored the objects with their right hand. Since the low-level motor and somatosensory response fields are lateralized and spatially localized, the fact that similar performance is observed across hemispheres suggests that more abstract information is shared between hemispheres (Smith and Goodale, 2013).

In addition to the somatosensory cortices, our searchlight analysis revealed that the patterns of LOC activation also allow the decoding of tactile object categories (Amedi et al., 2002; Saito et al., 2003). The predictive capacity of LOC is unlikely to be explained by low-level physical attributes such as shape, texture or weight, or by differences in hand movements used to explore each type of object. The LOC is a high-level visual region that is known to be related to multimodal processing of object shape and identity, and there is no evidence suggesting that LOC is engaged in the processing of low-level somatic information. Instead, there is a large body of previous findings that strongly support the notion that LOC encodes the identity of objects recognized by visual or somatic exploration (Amedi et al., 2002; Stilla and Sathian, 2008; Lucan et al., 2010; Masson et al., 2015; Erdogan et al., 2016; Peltier et al., 2007).

Anatomical evidence, from tracer studies in macaque monkeys, shows that somatosensory information reaches the temporal lobe through the inferior parietal lobe. Starting in the primary somatosensory cortices (areas 3a, 3b, 1 and 2), tactile activity then travels to the

superior (area 5) and inferior parietal lobe (areas 7a and 7b). The inferior parietal lobe then projects to the superior and inferior temporal lobes by means of the middle and inferior longitudinal fasciculi, respectively (Jones, 1969; Andersen et al., 1990; Distler et al., 1993; Seltzer and Pandya, 1994; Webster et al., 1994). The human homologs of these connections have been found using fiber-tracking techniques (Caspers et al., 2011; Schmahmann et al., 2007). Moreover, it has been recently proposed that LOC and the parietal cortices are part of a "grasping network" that generates purposeful hand actions such as tactile object recognition, both in monkeys and humans (Borra and Luppino, 2016; Borra et al., 2017).

There at least two explanations that can be contemplated in trying to understand the nature of the representation observed in LOC. One is that LOC contains an abstract representation of objects that can be elicited by any sensory modality. The second explanation is that LOC contains a visual representation of objects, and this visual representation can be evoked by different sensory modalities such as touch or audition (James et al., 2002; Zhang et al., 2004).

In a previous investigation we identified the cortical areas related to exploring and comparing the shape of objects explored with the hand, and we also found LOC activation (Rojas-Hortelano et al., 2014). A key experimental design in that study was that the participants never saw the objects, and their 3D shapes were pseudo-randomly created. Thus, we know that LOC is able to encode shapes that have never been seen. However, any object explored with the hand, familiar or not, can be visually represented as a combination of previously known shapes such as spheres or cubes. Therefore, a visual representation in LOC cannot be easily dismissed. Recent studies have found that the occipitotemporal cortex is able to represent object shape in blind people (Pietrini et al., 2004; Bonino et al., 2008; Peelen et al., 2014), and although this does not rule out a visual representation in sighted individuals, the results are consistent with the idea that LOC might encode an abstract representation of object identity. We speculate that the parietal cortices encode low level attributes of the objects such as texture and weight while LOC might be encoding shape and object identity. However, future research is needed to elucidate the specific role that the parietal and LOC cortices play in the identification of objects and object categories. Future experiments with an event-related design are also needed for the analysis of single trials. This would allow to compare correct versus incorrect behavioral responses and the neuronal activity underlying the decision-making component of the task.

As was brought to our attention by an anonymous reviewer the group accuracy map (Fig. 4) shows that the somatosensory orofacial region has significant predictive accuracy. This is an intriguing observation whose meaning we can only speculate about. The identification of objects could have triggered the imagery of the objects' name. Although this imagery process should have also recruited the orofacial motor cortex, it is important to note that the MVPA does not measure activation but makes use of the spatial patterns of activity. In this sense, the proximity of supramarginal gyrus and the orofacial cortices could have increased their combined predictive capacity.

What physical attributes the participants use to classify the objects is an interesting question. We approached this issue by performing hierarchical clustering on the dissimilarity matrix that results from the pairwise comparison of the distance between categories in the high-dimensional space. We failed to uncover any evident or meaningful classification. This result indicates that the categories we used did not systematically vary along a physical or perceptual axis.

CONCLUSION

Our investigation answered a simple but important question: tactile object categories can be decoded not only from the somatic and motor cortices, but also from what is likely a multimodal representation of objects located at the junction of the occipital and temporal lobes. How this abstract representation of objects emerges through learning, and how it is evoked by the low-level information arising from the sensory systems are fundamental questions that are intensely investigated but that we do not yet fully understand (Man et al., 2013).

Acknowledgments—We thank Edgar Bolaños, Leopoldo González and Erick Pasaye for their technical assistance, and Jessica M. González Norris for proofreading. We appreciate the comments and suggestions of Fernando Barrios and Sarael Alcauter. Raúl Hernández-Pérez is a doctoral student from Programa de Doctorado en Ciencias Biomédicas, Universidad Nacional Autónoma de México (UNAM) and received a fellowship (409258) from Consejo Nacional de Ciencia y Tecnología (CONACYT). This research was supported by Dirección del Personal Académico de la Universidad Nacional Autónoma de México (VdL: IN201115) and CONACYT (VdL: 254313, 247200, Fronteras de la Ciencia 245, LC: SSA/IMSS/ISSSTE-Conacyt 181508).

REFERENCES

Amedi A, Jacobson G, Hendler T, Malach R, Zohary E (2002) Convergence of visual and tactile shape processing in the human lateral occipital complex. Cereb Cortex 12(11):1202–1212.

Amedi A, Malach R, Hendler T, Peled S, Zohary E (2001) Visuo-haptic object-related activation in the ventral visual pathway. Nat Neurosci 4(3):324–330.

Andersen RA, Asanuma C, Essick G, Siegel RM (1990) Corticocortical connections of anatomically and physiologically defined subdivisions within the inferior parietal lobule. J Comp Neurol 296(1):65–113.

Aparicio PL, Issa E, DiCarlo JJ (2016) Neurophysiological organization of the middle face patch in macaque inferior temporal cortex. J Neurosci. http://dx.doi.org/10.1523/JNEUROSCI.0237-16.2016.

Bensmaia SJ, Denchev PV, Dammann JF, Craig JC, Hsiao SS (2008) The representation of stimulus orientation in the early stages of somatosensory processing. J Neurosci 28(3):776–786.

Bodegård A, Geyer S, Grefkes C, Zilles K, Roland PE (2001) Hierarchical processing of tactile shape in the human brain. Neuron 31(2):317–328.

Bonino D, Ricciardi E, Sani L, Gentili C, Vanello N, Guazzelli M, Pietrini P (2008) Tactile spatial working memory activates the

dorsal extrastriate cortical pathway in congenitally blind individuals. Arch Ital Biol 146(3–4):133–146.
Borra E, Gerbella M, Rozzi S, Luppino G (2017) The macaque lateral grasping network: a neural substrate for generating purposeful hand actions. Neurosci Biobehav Rev.
Borra E, Luppino G (2016) Functional anatomy of the macaque temporo-parieto-frontal connectivity. Cortex.
Caspers S, Eickhoff SB, Rick T, von Kapri A, Kuhlen T, Huang R, Zilles K (2011) Probabilistic fibre tract analysis of cytoarchitectonically defined human inferior parietal lobule areas reveals similarities to macaques. Neuroimage 58(2):362–380.
Chen J, Reitzen SD, Kohlenstein JB, Gardner EP (2009) Neural representation of hand kinematics during prehension in posterior parietal cortex of the macaque monkey. J Neurophysiol 102 (6):3310–3328.
Connolly AC, Sha L, Guntupalli JS, Oosterhof N, Halchenko YO, Nastase SA, Haxby JV (2016) How the human brain represents perceived dangerousness or "predacity" of animals. J Neurosci 36 (19):5373–5384.
Distler C, Boussaoud D, Desimone R, Ungerleider LG (1993) Cortical connections of inferior temporal area TEO in macaque monkeys. J Comp Neurol 334(1):125–150.
Erdogan G, Chen Q, Garcea FE, Mahon BZ, Jacobs RA (2016) Multisensory part-based representations of objects in human lateral occipital cortex. J Cogn Neurosci.
Etzel JA, Zacks JM, Braver TS (2013) Searchlight analysis: promise, pitfalls, and potential. Neuroimage 78:261–269.
Fitzgerald PJ, Lane JW, Thakur PH, Hsiao SS (2006) Receptive field properties of the macaque second somatosensory cortex: representation of orientation on different finger pads. J Neurosci 26(24):6473–6484.
Freeman J, Simoncelli EP (2011) Metamers of the ventral stream. Nat Neurosci 14(9):1195–1201.
Friston KJ, Buechel C, Fink GR, Morris J, Rolls E, Dolan RJ (1997) Psychophysiological and modulatory interactions in neuroimaging. Neuroimage 6(3):218–229.
Gardner EP, Babu KS, Reitzen SD, Ghosh S, Brown AS, Chen J, Ro JY (2007) Neurophysiology of prehension. I. Posterior parietal cortex and object-oriented hand behaviors. J Neurophysiol 97 (1):387–406.
Ghazanfar AA, Schroeder CE (2006) Is neocortex essentially multisensory? Trends Cogn Sci 10(6):278–285.
Grill-Spector K, Kourtzi Z, Kanwisher N (2001) The lateral occipital complex and its role in object recognition. Vision Res 41 (10):1409–1422.
Hanke M, Halchenko YO, Sederberg PB, Hanson SJ, Haxby JV, Pollmann S (2009) PyMVPA: a python toolbox for multivariate pattern analysis of fMRI data. Neuroinformatics 7(1):37–53.
Haxby JV, Connolly AC, Guntupalli JS (2014) Decoding neural representational spaces using multivariate pattern analysis. Annu Rev Neurosci 37:435–456.
Haxby JV, Guntupalli JS, Connolly AC, Halchenko YO, Conroy BR, Gobbini MI, Hanke M, Ramadge PJ (2011) A common, high-dimensional model of the representational space in human ventral temporal cortex. Neuron 72(2):404–416.
Iwamura Y (1998) Hierarchical somatosensory processing. Curr Opin Neurobiol 8(4):522–528.
Ishai A, Ungerleider LG, Haxby JV (2000) Distributed neural systems for the generation of visual images. Neuron 28(3):979–990.
James TW, Humphrey GK, Gati JS, Servos P, Menon RS, Goodale MA (2002) Haptic study of three-dimensional objects activates extrastriate visual areas. Neuropsychologia 40(10):1706–1714.
Jones EG (1969) Interrelationships of parieto-temporal and frontal cortex in the rhesus monkey. Brain Res 13(2):412–415.
Kassuba T, Klinge C, Hölig C, Menz MM, Ptito M, Röder B, Siebner HR (2011) The left fusiform gyrus hosts trisensory representations of manipulable objects. Neuroimage 56 (3):1566–1577.
Kiani R, Esteky H, Mirpour K, Tanaka K (2007) Object category structure in response patterns of neuronal population in monkey inferior temporal cortex. J Neurophysiol 97(6):4296–4309.
Kim JK, Zatorre RJ (2011) Tactile–auditory shape learning engages the lateral occipital complex. J Neurosci 31(21):7848–7856.
Kim SS, Gomez-Ramirez M, Thakur PH, Hsiao SS (2015) Multimodal interactions between proprioceptive and cutaneous signals in primary somatosensory cortex. Neuron 86(2):555–566.
Kourtzi Z, Connor CE (2011) Neural representations for object perception: structure, category, and adaptive coding. Annu Rev Neurosci 34:45–67.
Lacey S, Sathian K (2014) Visuo-haptic multisensory object recognition, categorization, and representation. Front Psychol 5:730.
Lehky SR, Kiani R, Esteky H, Tanaka K (2014) Dimensionality of object representations in monkey inferotemporal cortex. Neural Comput 26(10):2135–2162.
Lucan JN, Foxe JJ, Gomez-Ramirez M, Sathian K, Molholm S (2010) Tactile shape discrimination recruits human lateral occipital complex during early perceptual processing. Hum Brain Mapp 31(11):1813–1821.
Man K, Damasio A, Meyer K, Kaplan JT (2015) Convergent and invariant object representations for sight, sound, and touch. Hum Brain Mapp 36(9):3629–3640.
Man K, Kaplan J, Damasio H, Damasio A (2013) Neural convergence and divergence in the mammalian cerebral cortex: From experimental neuroanatomy to functional neuroimaging. J Comp Neurol 521(18):4097–4111.
Masson HL, Bulthé J, de Beeck HPO, Wallraven C (2015) Visual and haptic shape processing in the human brain: unisensory processing, multisensory convergence, and top-down influences. Cereb Cortex. http://dx.doi.org/10.1093/cercor/bhv170.
McKee JL, Riesenhuber M, Miller EK, Freedman DJ (2014) Task dependence of visual and category representations in prefrontal and inferior temporal cortices. J Neurosci 34(48):16065–16075.
Meyers EM, Freedman DJ, Kreiman G, Miller EK, Poggio T (2008) Dynamic population coding of category information in inferior temporal and prefrontal cortex. J Neurophysiol 100 (3):1407–1419.
Mollazadeh M, Aggarwal V, Thakor NV, Schieber MH (2014) Principal components of hand kinematics and neurophysiological signals in motor cortex during reach to grasp movements. J Neurophysiol 112(8):1857–1870.
Peelen MV, He C, Han Z, Caramazza A, Bi Y (2014) Nonvisual and visual object shape representations in occipitotemporal cortex: evidence from congenitally blind and sighted adults. J Neurosci 34 (1):163–170.
Peltier S, Stilla R, Mariola E, LaConte S, Hu X, Sathian K (2007) Activity and effective connectivity of parietal and occipital cortical regions during haptic shape perception. Neuropsychologia 45 (3):476–483.
Pereira F, Botvinick M (2011) Information mapping with pattern classifiers: a comparative study. Neuroimage 56(2):476–496.
Peters RM, Staibano P, Goldreich D (2015) Tactile orientation perception: an ideal observer analysis of human psychophysical performance in relation to macaque area 3b receptive fields. J Neurophysiol 114(6):3076–3096.
Pietrini P, Furey ML, Ricciardi E, Gobbini MI, Wu WHC, Cohen L, Haxby JV (2004) Beyond sensory images: Object-based representation in the human ventral pathway. Proc Natl Acad Sci U S A 101(15):5658–5663.
Podrebarac SK, Goodale MA, Snow JC (2014) Are visual texture-selective areas recruited during haptic texture discrimination? Neuroimage 94:129–137.
Proklova D, Kaiser D, Peelen MV (2016) Disentangling representations of object shape and object category in human visual cortex: the animate-inanimate distinction. J Cogn Neurosci.
Pruszynski JA, Johansson RS (2014) Edge-orientation processing in first-order tactile neurons. Nat Neurosci 17(10):1404–1409.
Reed CL, Shoham S, Halgren E (2004) Neural substrates of tactile object recognition: an fMRI study. Hum Brain Mapp 21 (4):236–246.

Rojas-Hortelano E, Concha L, de Lafuente V (2014) The parietal cortices participate in encoding, short-term memory, and decision-making related to tactile shape. J Neurophysiol 112 (8):1894–1902.

Saito DN, Okada T, Morita Y, Yonekura Y, Sadato N (2003) Tactile–visual cross-modal shape matching: a functional MRI study. Cognitive Brain Research 17(1):14–25.

Schmahmann JD, Pandya DN, Wang R, Dai G, D'arceuil HE, de Crespigny AJ, Wedeen VJ (2007) Association fibre pathways of the brain: parallel observations from diffusion spectrum imaging and autoradiography. Brain 130(3):630–653.

Sathian K (2016) Analysis of haptic information in the cerebral cortex. J Neurophysiol 116(4):1795–1806.

Seltzer B, Pandya DN (1994) Parietal, temporal, and occipita projections to cortex of the superior temporal sulcus in the rhesus monkey: A retrograde tracer study. J Comp Neurol 343 (3):445–463.

Smith FW, Goodale MA (2013) Decoding visual object categories in early somatosensory cortex. Cereb Cortex. http://dx.doi.org/10.1093/cercor/bht292.

Snow JC, Strother L, Humphreys GW (2014) Haptic shape processing in visual cortex. J Cogn Neurosci 26(5):1154–1167.

Stilla R, Sathian K (2008) Selective visuo-haptic processing of shape and texture. Hum Brain Mapp 29(10):1123–1138.

Thakur PH, Bastian AJ, Hsiao SS (2008) Multidigit movement synergies of the human hand in an unconstrained haptic exploration task. J Neurosci 28(6):1271–1281.

Watanabe T, Kimura HM, Hirose S, Wada H, Imai Y, Machida T, Konishi S (2012) Functional dissociation between anterior and posterior temporal cortical regions during retrieval of remote memory. J Neurosci 32(28):9659–9670.

Webster MJ, Bachevalier J, Ungerleider LG (1994) Connections of inferior temporal areas TEO and TE with parietal and frontal cortex in macaque monkeys. Cereb Cortex 4(5):470–483.

Yamada H, Yaguchi H, Tomatsu S, Takei T, Oya T, Seki K (2016) Representation of afferent signals from forearm muscle and cutaneous nerves in the primary somatosensory cortex of the macaque monkey. PLoS One 11(10):e0163948.

Yau JM, Pasupathy A, Fitzgerald PJ, Hsiao SS, Connor CE (2009) Analogous intermediate shape coding in vision and touch. Proc Natl Acad Sci U S A 106(38):16457–16462.

Yau JM, Connor CE, Hsiao SS (2013) Representation of tactile curvature in macaque somatosensory area 2. J Neurophysiol 109 (12):2999–3012.

Yau JM, Kim SS, Thakur PH, Bensmaia SJ (2016) Feeling form: the neural basis of haptic shape perception. J Neurophysiol 115 (2):631–642.

Yildirim I, Jacobs RA (2013) Transfer of object category knowledge across visual and haptic modalities: Experimental and computational studies. Cognition 126(2):135–148.

Zhang M, Weisser VD, Stilla R, Prather SC, Sathian K (2004) Multisensory cortical processing of object shape and its relation to mental imagery. Cogn Affect Behav Neurosci 4(2):251–259.

(Received 10 December 2016, Accepted 24 March 2017)
(Available online 02 April 2017)